Journal of Achievements in Materials and Manufacturing Engineering
VOLUME 43
ISSUE 1
November
2010

Effect of deep cryogenic treatment on substructure of HS6-5-2 high speed steel

J. Jeleńkowski, A. Ciski*, T. Babul
Institute of Precision Mechanics, ul. Duchnicka 3, 01-796 Warsaw, Poland
* Corresponding author: E-mail address: ciski@imp.edu.pl

Received 11.09.2010; published in revised form 01.11.2010

Materials

ABSTRACT

Purpose: The purpose of this study was using of transmission electron microscopy (TEM) and differential scanning calorimetry (DSC) in order to reveal the changes in substructure of speed steel made with deep cryogenic treatment (DCT), in comparison with substructure formed by conventional heat treatment for secondary hardness.
Design/methodology/approach: The HS6-5-2 high speed steel was heat treated in a conventional mode for secondary hardness or was processed in a mode with use of DCT, with and without next tempering. Transmission electron microscopy and scanning electron microscopy observations were carried out. Studies of thermal stability in range of temperatures from -196 °C to 400 °C were performed using differential scanning calorimetry (DSC).
Findings: Observations made with aid of SEM-TEM microscope revealed the presence of high density of globular clusters situated at dislocations, and precipitations of the fine carbide plates, located in twinned crystals of martensite. Thermal analysis (DSC) showed an occurrence of higher exothermic effects in specimens treated with use of DCT, than in specimens heat treated conventionally. In steel samples after quenching and DCT the additional exothermic effect was observed. Electron diffraction in TEM studies of these specimens allowed to observe reflections of which indexing exhibited that the precipitated carbide phase has crystallographic structure of B1 type.
Research limitations/implications: Extremely high dispersion of carbide phases and a high state of stress that accompanies the stage of precipitation, make difficult the identification of the lattice structure of precipitations, its crystallographic relationships and the degree of coherence with the matrix. Identification of the type of carbides (ε, η, B1, and others) and their coherence with matrix become time-consuming. This important issue requires detailed studies using high-resolution microscopes. Conditions of the early stage of the precipitation process affect the stability of induced strengthening and service-life of tools.
Practical implications: Research of HS6-5-2 high speed steel allowed concluding that DCT, besides refinement of martensite grain size, causes an increase of quantity of sites for nucleation of clusters, in which during tempering the B1 carbides are formed. These fine, coherent with matrix and stable carbides are found to be responsible for enhancement of toughness and wear resistance of HSS tools.
Originality/value: The issue of DCT is a niche topic in Poland, there are no detailed studies on the changes taking place during this process.
Keywords: Tool materials; High speed steel; Deep cryogenic treatment; Carbides

Reference to this paper should be given in the following way:
J. Jeleńkowski, A. Ciski, T. Babul, Effect of deep cryogenic treatment on substructure of HS6-5-2 high speed steel, Journal of Achievements in Materials and Manufacturing Engineering 43/1 (2010) 80-87.

1. Introduction

Nowadays, forming of the special carbides is considered as consisting of two stages: 1) formation of clusters – zones consisting of carbide forming elements and carbon; and 2) the rebuilding of these areas into a special carbide. The first step is a spinodal decomposition and this mechanism underlies the observed structural phenomena [1, 2]. With the increase of tempering temperature and time, grow only clusters not connected with defects of the crystalline structure of the matrix, thus these located on planes $\{100\}_\alpha$. Clusters transform into the lamellar forms, probably by the dissolution of smaller ones. The globules at dislocations, i.e. in small areas, do not get a more stable shape needed for further growth. Also a random orientation of the dislocations doesn't allow clusters taking the preferred direction of growth [3, 4].

Important role in the formation of special carbides play vacancies [5]. Vacancies are causing that at temperature below 250 °C the least stable carbides are formed, for example ε–Fe_3C, but the precipitation of a coherent carbide α'–$Fe_{16}C_2$ at temperature lower than 100 °C is also possible, when the substitutional elements are still not mobile. In high speed steels, in addition to mentioned carbides, special B1 carbides and η-carbides with a regular structure consisting of 96 metallic atoms (Fe atoms and the metals of V and VI group) and 16 carbon atoms, can be formed [6].

Identification of the special carbide is difficult because of their dispersion, and the fact that their final structure may be different. Carbides are phases with a very wide area of homogeneity, depletion of carbon atoms and elevated concentration of vacancies, in which with a decrease of carbon concentration, there is ability for substantial arrangement.

It was stated [1, 2, 3, 4] that the increase in arrangement should result in achieving of B1 crystal structure, in which the volume of elementary cell increases 8 times, as compared with the baseline one. The cell contains 32 vanadium atoms and 32 ion nodes, occupied by the carbon and vacancies. This is the reason why the VC may have a regular (B1), rhombic or rhombohedral lattice structure, and may contain up to 50 % of W and Mo, and up to 25 % of Cr.

The literature information states that deep cryogenic treatment causes increase in hardness, toughness and wear resistance [7–9]. During tempering the highly alloyed retained austenite with carbide precipitations transforms into secondary martensite [10].

The purpose of this study was using of transmission electron microscopy (TEM) and differential scanning calorimetry (DSC) in order to reveal the changes in substructure of speed steel made with DCT, in comparison with substructure formed after conventional heat treatment for secondary hardness.

2. Material, work methodology

Research was conducted on HS6-5-2 high-speed steel. Chemical composition of samples was analysed with aid of Analytical Spectrometer Foundry Master 01D0058. The results of measurements are given in Table 1.

Transmission electron microscopy and scanning electron microscopy analyses were conducted with aid of scanning-transmission electron microscope HITACHI HD2700, equipped with an energy-dispersive X-Ray spectrometer (EDS), allowing spectral analysis of chemical composition in areas with a diameter of 0.5 mm. Elemental mapping was also performed. Studies of thermal stability in range of temperatures from -196 °C to 400 °C were performed using differential scanning calorimetry (DSC), with aid of the Parkin Elmer calorimeter. The samples were cooled down and heated up at a rate of 10 °C/min.

Table 1.
Chemical composition of samples

	Chemical composition, weight %							
	C	Si	Mn	Cr	Mo	V	W	Co
Typical composition	0.82-0.92	≤0.5	≤0.4	3.5÷4.5	4.5-5.5	1.7-2.1	6.0-7.0	≤0.5
Actual composition	0.83	0.31	0.26	4.25	4.2	1.78	6.08	0.34

For SEM and TEM investigations a foils cut from the rode samples (diameter of 3 mm) were used. The same rods were used for preparation of disc samples (diameter of 3 mm) used in calorimetric studies. DSC samples were cut using electric spark method and had mass of 10 mg. All samples were tested in three modes of heat treatment. Treatment modes, obtained values of hardness and ASTM grain numbers are summarized in Table 2.

Table 2.
Routes of heat treatment, obtained values of hardness and ASTM primary austenite grain numbers of samples

Mode	Route of heat treatment	Hardness	ASTM grain no.
A	Austenitizing (1200 °C) + Quenching + Tempering (550 °C, 2 h)	936 HV1	10-11
B	Austenitizing (1200 °C) + Quenching + DCT (-180 °C, 24 h)	863 HV1	10-11
C	Austenitizing (1200 °C) + Quenching + DCT (-180 °C, 24 h) + Tempering (550 °C, 2 h)	902 HV1	10-11

3. Results of research

In all examined samples, regardless of the applied heat treatment, presence of Fe_α (martensite), Fe_γ (austenite), M_6C (Fe_3W_3C or Fe_4W_2C) and VC was identified with aid of XRD method. The relatively lowest intensity of diffraction lines from the phase components, except for Fe_γ and M_6C, was observed in the mode of heat treatment B, while the highest was observed, except for Fe_γ, in the mode C. Qualitative analysis of the diffraction line positions of the Fe_α lattice as a function of the angle of diffraction of steel heat treated in modes A, B and C, showed that the parameter of Fe_α unit cell was the highest after the heat treatment for secondary hardness without deep cryogenic treatment (mode A), and the lowest after the DCT and heating up to room temperature (mode B).

3.1. SEM/TEM imaging

Imaging of the structure using TEM/SEM showed that in each one of the heat treatment modes, martensite has the lamellar-lenticular structure, internally twinned, sometimes with midribs, with the fairly evenly distributed dislocations. Morphology of martensite of steel tempered for secondary hardness is characterized by a partial disappearance of twins and midribs. However the quantity and size of primary carbides remain the same. Primary austenite grains size (8–10 μm) corresponds to the grain size number 10–11 on the ASTM scale. Carbides of the spherical shape (VC) and a diameter of about 1 μm are generally located within the martensite grains, whereas these oval-shaped (M_6C), with a diameter of about two times higher, at the grain boundaries. In the mode A samples plates have length of about 1–2 μm and width of about 0.3–0.4 μm, while in deep cryogenically treated samples (modes B and C) these dimensions are an order of magnitude shorter and thinner (Figs. 1-3).

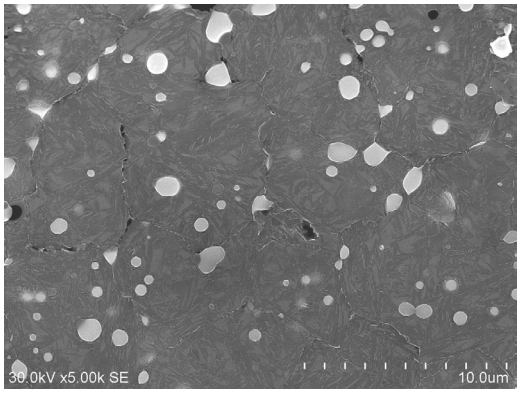

Fig. 1. SEM micrograph of sample heat treated in mode A

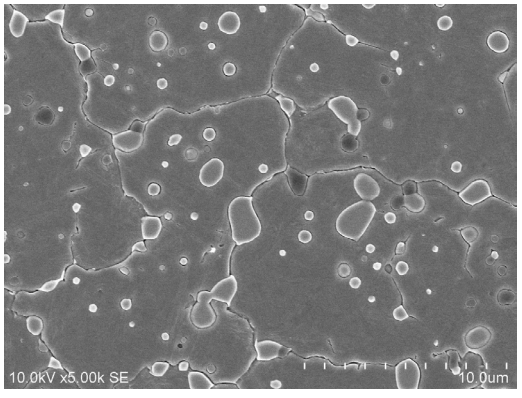

Fig. 2. SEM micrograph of sample heat treated in mode B

In the matrix of samples heat treated in mode A, there are present clusters-globules with a diameter of 10–15 nm located at dislocations, and plates situated at the grain boundaries and within the martensite twins, with a thickness of about 10–15 nm and length up to about 100 nm. In mode B, globules and plates have clearly defined contours. Local configurations of some plates resemble morphology of the tweed-like structure, i.e. the morphology of precipitations formed by the spinodal decomposition. In mode C, a considerable refinement and morphology of the martensite seems to be similar to that observed in mode A (Figs. 4-6).

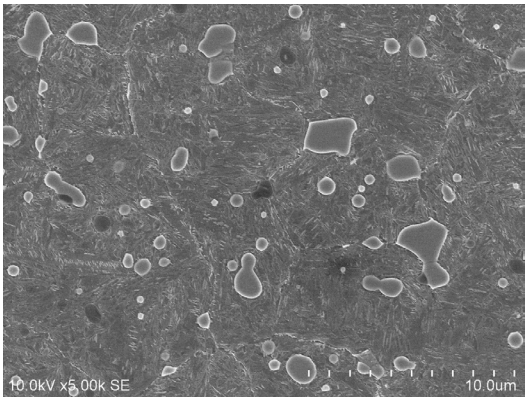

Fig. 3. SEM micrograph of sample heat treated in mode C

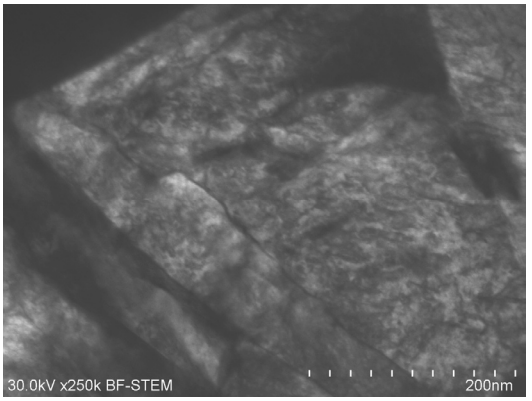

Fig. 4. TEM micrograph of sample heat treated in mode A

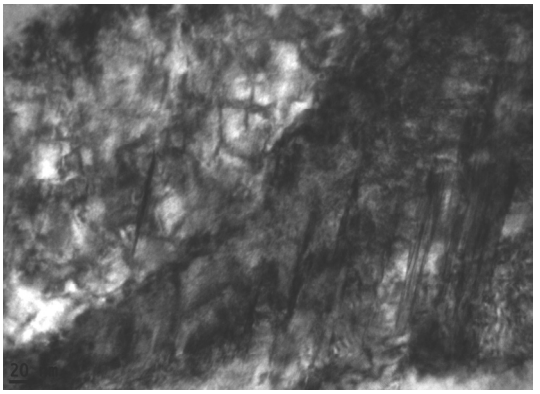

Fig. 5. TEM micrograph of sample heat treated in mode B

3.2. TEM diffraction

When comparing the samples heat treated in mode C with those from the mode A, increased intensity of the reflections from the carbides was noted. From the reflections of the matrix the streaks in the $<110>_{\alpha}$ direction are formed and linked along the $<100>_{\alpha}$ direction, there is also a diffuse scattering around them (Figs. 7, 9). This demonstrates the dissolution of some precipitations, what is also confirmed by the increase of the lattice parameter of the matrix.

When comparing samples from mode B and C, it can be concluded that already when heating up from cryogenic treatment temperature to room temperature, and then at the time of tempering, the evolution of clusters from globules at dislocations to the plate precipitations on planes $\{100\}_{\alpha}$ occurs.

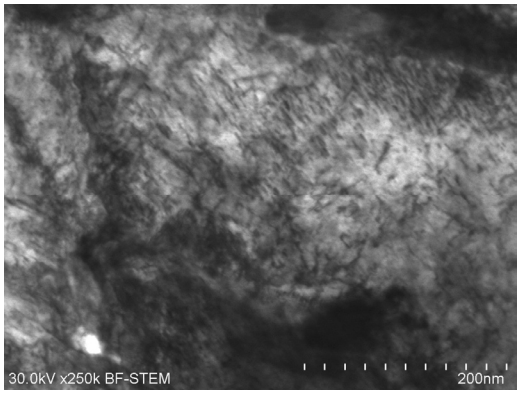

Fig. 6. TEM micrograph of sample heat treated in mode C

a) b)

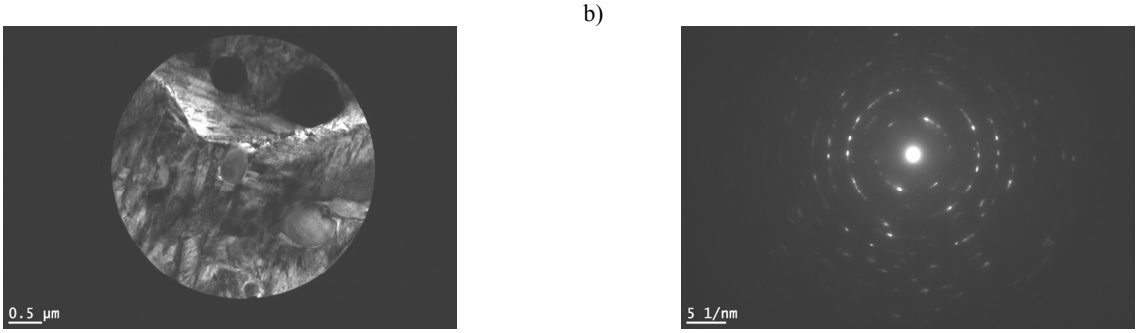

Fig. 7. TEM micrograph (a) and diffraction pattern (b) of sample heat treated in mode A

a) b)

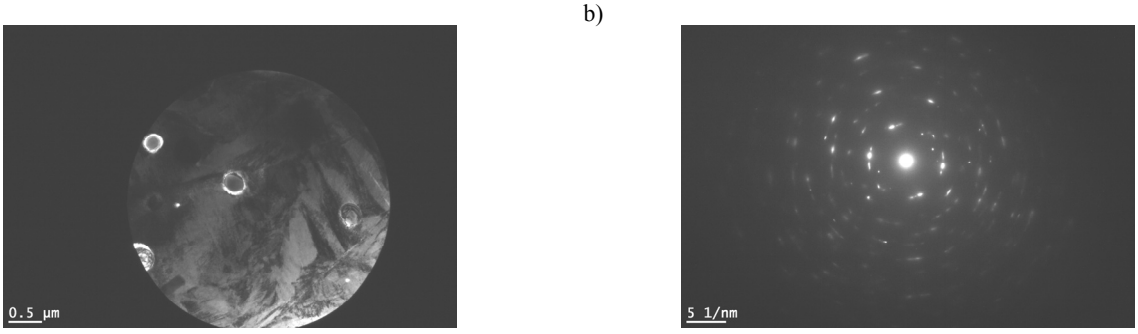

Fig. 8. TEM micrograph (a) and diffraction pattern (b) of sample heat treated in mode B

a) b)

Fig. 9. TEM micrograph (a) and diffraction pattern (b) of sample heat treated in mode C

At the diffractograms of steel heat treated in mode B (Fig. 8) appear more contrasting and incomplete reflections, which indexing showed that they come from the B1 carbide phase. Lack of proper crystallographic orientation consistence with the martensite, similar to Bain relationship, may be due to slight tetragonality and lack of matching of $<001>_{\alpha}$ and $<110>_{c}$ directions. Diffraction studies confirm the presence of (in addition to cementite) special carbides in the form of plates arranged on the planes $\{100\}_{\alpha}$ (Fig. 10).

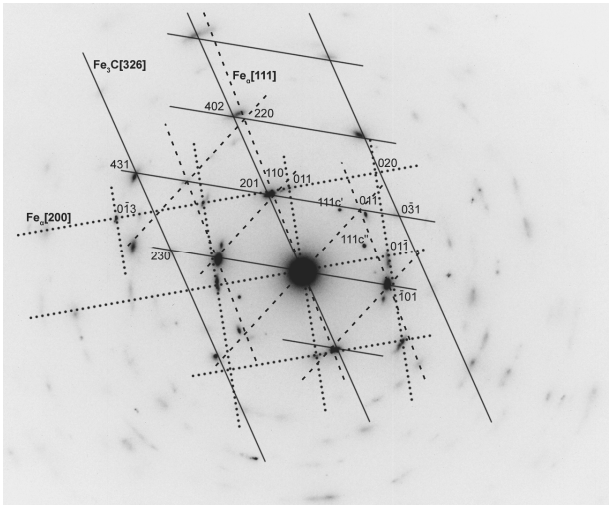

Fig. 10. Indexed pattern of sample heat treated in mode B3.3. Energy Dispersive X-ray Spectroscopy (EDS) with elemental mapping

3.3. Energy Dispersive X-ray Spectroscopy (EDS) with elemental mapping

For comparative qualitative analysis of the chemical composition of carbide phases energy dispersive X-ray spectroscopy and elemental mapping were used. Points of measurements are shown in Figure 11, while obtained results are presented in Table 3.

Table 3.
Chemical composition, weight %

Mode	C	V	Cr	Fe	Mo	W
A	10.52	4.74	3.51	60.53	5.41	11.07
B	4.93	2.38	3.10	74.71	5.16	9.72
C	5.98	6.13	3.78	71.37	4.45	8.28

As can be seen from Table 3, in modes A and C, spheroidal VC carbides present in the matrix, contain also molybdenum, tungsten and chromium. In two to three times larger oval M_6C carbides, in addition to tungsten content, the molybdenum and small amount of chromium is present. In comparison with the sample after DCT and tempering (mode B) there is lower content of V, Cr and Mo. The content of tungsten is also lower than after standard heat treatment (Figs. 12-14).

a)

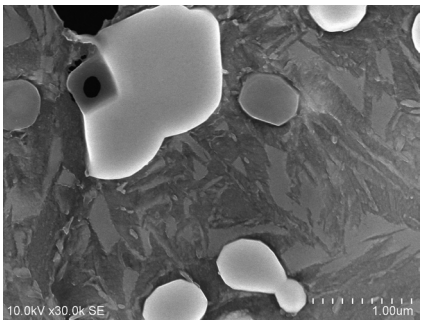

b)

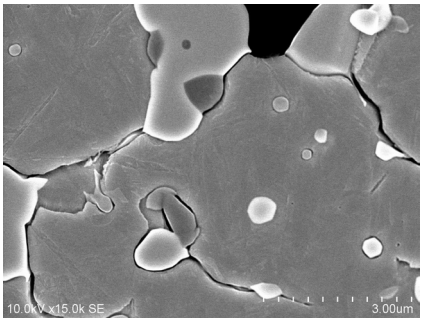

c)

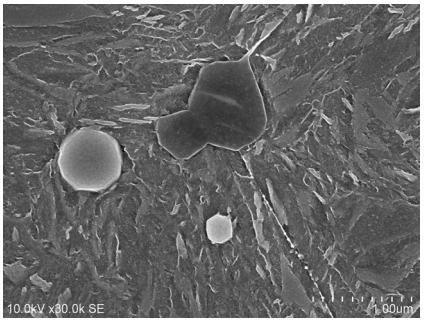

Fig. 11. Places of measurements of chemical composition of samples heat treated in mode A (a), B (b) and C (c)

In samples heat treated in mode B, M_6C carbides contain a considerable amounts of tungsten and molybdenum, but doesn't contain vanadium. In VC carbides there is the highest percentage of vanadium. Chromium is evenly distributed in the matrix. In comparison with mode A there is a lesser amount of tungsten, molybdenum and chromium (Fig. 13).

In the mode C, in M_6C carbides there is a relatively higher amount of W and Mo; and lesser amount of V and Fe. Carbides are finer, and just like plates, very evenly distributed in the matrix (Fig. 14).

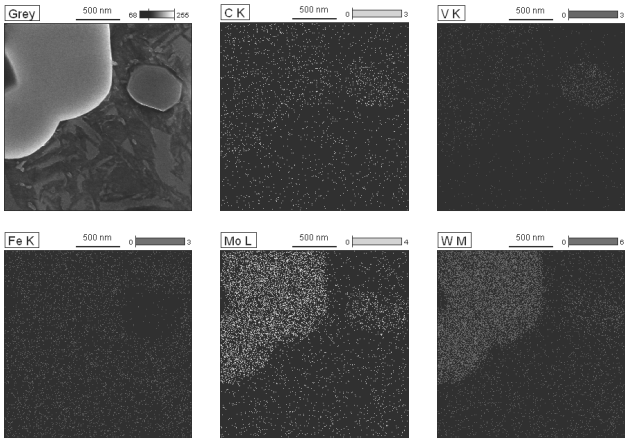

Fig. 12. Results of elemental mapping of samples heat treated in mode A

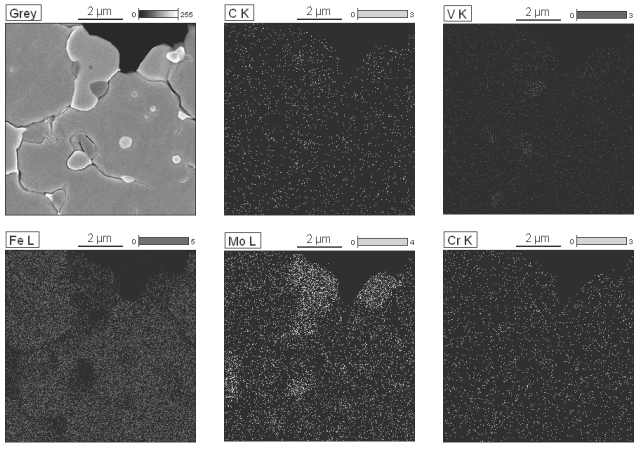

Fig. 13. Results of elemental mapping of samples heat treated in mode B

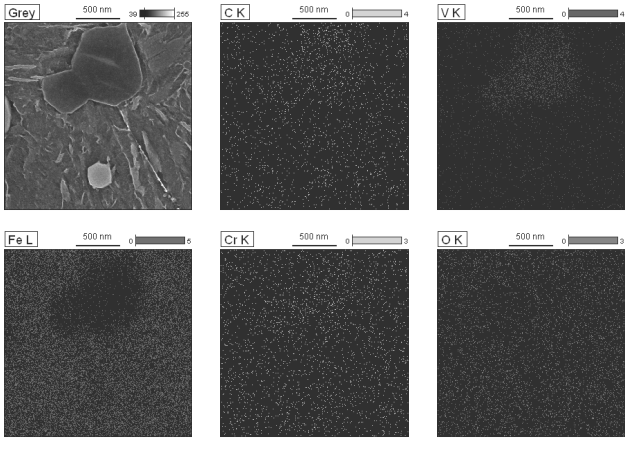

Fig. 14. Results of elemental mapping of samples heat treated in mode C

3.4. Differential scanning calorimetry

All samples were subjected to the identical thermal cycle: cooling down from the room temperature to LN_2 temperature, soaking for 5 minutes at cryogenic temperature, heating up to 400 °C and cooling down back to the room temperature. The samples were cooled down and heated up at a rate of 10 °C/min. Exemplary calorimetric measurements are shown in Figure 15, while the results of the analysis are summarized in Table 4.

Table 4.
Results of calorimetric examinations (DSC)

Mode	Temperature °C	Heat flow J/g
A	10.5 (-27.3)	0.29
	128.7 (100.8)	0.64
	283.5 (212.4)	2.10
B	7.8 (-70.5)	1.79
	148.3 (102.2)	1.45
	277.9 (256.4)	0.23
	329.1 (306.4)	0.52
C	1.2 (-98.3)	0.65
	136.4 (100.0)	0.43
	278.7 (258.6)	0.13

In the brackets are given the temperatures of a beginning of the exothermic effect during heating up from the temperature of -196 °C to 400 °C. During cooling down of the samples from the room temperature to -196 °C, thermal effects were not observed.

As it is apparent from the thermograms and the data contained in Table 4, the samples heat treated for secondary hardness (modes A and C), reveal appearance of 3 peaks. The third peak in mode A shows an order of magnitude greater amount of generated heat. In steel sample heat treated in mode B, also the additional peak was observed (329 °C, Table 4), wherein the first three peaks, as compared to the mode A and C, almost didn't change their position on the axis of temperature. The first two low-temperature peaks were energetically richer.

The temperature range at which the exothermic thermal effects were recorded indicates that these effects are connected with the diffusion of carbon atoms. Thermal effect related to the first, the lowest temperature peak, reveals the zonal stage of forming of clusters, i.e. the diffusion of carbon atoms into the clusters of carbide forming elements. The second peak may be dominated by the change of shape of clusters from globular to disc form of B1 carbides, what is distinctly illustrated by two first peaks of samples heat treated in mode B.

Thermal effects recorded at a temperature above 250 °C, especially at temperature higher than 300 °C, indicate dissolution of cementite and diffusion of substitutional elements into carbide phases, supporting the precipitation of more stable B1 phase and contributing to its stabilization. It should be noted that in the samples heat treated in A and C modes, processes of cementite dissolution didn't occur, whereas the processes of nucleation and growth of special carbides were repeated.

a)

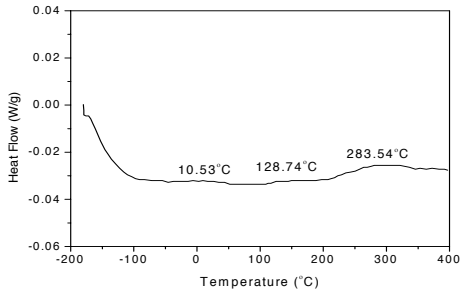

b)

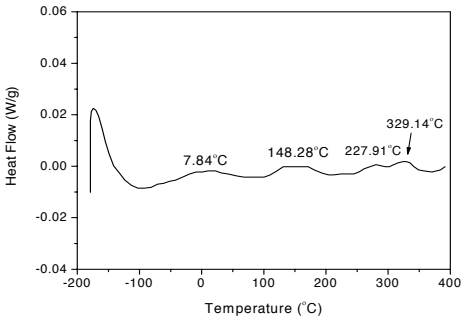

c)

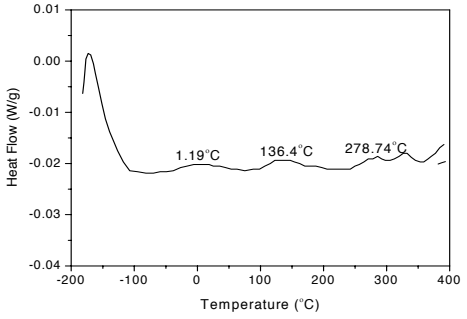

Fig. 15. DSC thermograms of samples heat treated in mode A (a), B (b) and C (c)

4. Summary and discussion

TEM imaging of the structure showed that the martensite obtained after quenching, deep cryogenic treatment and heating up to the ambient temperature, has a lamellar-lenticular structure, internally twinned, with very high density of dislocations. At dislocations, inside martensite plates and at the grain boundaries there are present globular shaped clusters with the size of a few nanometers. In martensite twins the clusters, or already formed B1 carbides plates, are arranged on $\{100\}_\alpha$ planes.

Morphology of martensite of steel tempered for secondary hardness is characterized by a disappearance of twins and midribs. In deep cryogenically treated samples dimensions of the martensite plates are almost an order of magnitude shorter and thinner. The size of primary austenite grains and size of precipitations of ledeburitic M_6C and VC carbides remain unchanged. Qualitative assessment (elemental mapping) of the concentration of atoms of alloying elements in carbides indicates that this concentration (with the exception of tungsten) is higher after the deep cryogenic treatment.

In the clusters and surrounding matrix there is a high stress state deforming the lattice structures, thus revealing the contours of the globules. The carbide lattice type is imposed by the steel matrix to minimize stresses. Coherent or semi-coherent with the matrix crystal B1 carbide structure decreases the carbide phase volume changes in relation to the matrix, therefore also reduces the stress state in the carbide and matrix.

When comparing stage C to B it can be concluded that during tempering occurs the evolution of clusters from globular shapes located at dislocations to the plate precipitations on close-packed lattice planes. This process in the modes of treatment A and C was not completed. Indexing of reflections of reciprocal lattice of samples heat treated in mode B confirm that carbides precipitating during heating up from cryogenic temperature to room temperature have structure of B1 type. There are also present reflections from cementite. In contrast to the mode B, in mode C on the TEM images there are observed almost identical plates parallel to $\{100\}_\alpha$.

The nature of the calorimetric curve is consistent with the precipitation sequence. Two first thermal effects are probably connected with the creation of zones. The highest exothermic effect at 270–320 °C is associated with dissolution of cementite and precipitation of a more stable phase B1, remaining until the range of the secondary hardness effect.

5. Conclusions

Deep cryogenic treatment doesn't alter the amount, size and distribution of special carbides, whereas it refines the substructure of martensite laths and plates. The rate of reduction of size is about ten times (about one order of magnitude).

In the heat treated for secondary hardness steel, with or without DCT, at dislocations there are present globular clusters with the size of a few nanometers, while at the boundaries of transformation twins and inside of the twins there are plates or discs located on $\{100\}_\alpha$ planes. As it was stated during electron diffraction in TEM investigations, they are carbides with B1 lattice structure.

Calorimetric recordings showed that some amount of heat was released already at negative temperature. During tempering the evolution of clusters-globules occurs, from the shape of the globules at dislocations to plate precipitations at close-packed lattice planes. Used in the studies times and temperatures of the heat treatment processes, with or without DCT, didn't lead to completing the evolution of clusters to special carbides.

References

[1] R. Collongues, La non-stoechiometrie, Masson, Paris, 1971.
[2] A. Inoue, S. Arakawa, T. Masumoto, In Situ Transformation of Cementite to M_7C_3 and Internal Defects of M_7C_3 in High Carbon-Chromium Steel by Tempering, Transactions of the Japan Institute of Metals 19/1 (1978) 11-17.

[3] A.G. Khachaturyan, The Theory of Phase Transformations and the Structure of Solid Solutions, Moskva: Nauka, Moscow, 1974 (in Russian).
[4] G.V. Kurdyumov, L.M. Utevskii, R.I. Entin, Transformations in iron and steel, Moskva: Nauka, Moscow, 1977 (in Russian).
[5] Yu.I. Ustinovshchikov, Secondary Hardening of Structural Alloy Steels, Moskva: Metallurgiya, Moscow, 1982 (in Russian).
[6] N.F. Lashko, L.V. Zaslavskaya, M.N. Kozlova, Physocochemical Phase Analysis of Steels and Alloys, Moskva: Metallurgiya, Moscow, 1978 (in Russian).
[7] D.N. Collins, Cryogenic treatment of tool steels, Advanced Materials and Processes 12 (1998) 23-29.
[8] F. Meng, K. Tagashira, R. Azuma, H. Sohma, Role of Eta-carbide Precipitations in the Wear Resistance Improvement of Fe-12Cr-Mo-V-1,4C Tool Steel by Cryogenic Treatment, ISIJ International 34 (1994) 205-210.
[9] D. Yun, L. Xiaoping, X. Hongshen, Deep-cryogenic treatment of high speed steel and its mechanism, Heat Treatment of Metals 3 (1988) 55-59.
[10] F. Cajner, V. Leskovsek, D. Landek, H. Cajner, Effect of Deep-Cryogenic Treatment on High Speed Steel Properties, Materials end Manufacturing Processes 24 (2009) 743-746.